
Article:
Tomlinson, S.E., Carre, M.J. orcid.org/0000-0003-3622-990X, Lewis, R. et al. (1 more author) (2011) Human finger contact with small, triangular ridged surfaces. Wear, 271 (9-10). pp. 2346-2353. ISSN 0043-1648

https://doi.org/10.1016/j.wear.2010.12.055

Human finger contact with small, triangular ridged surfaces

S. E. Tomlinson[1], M. J. Carré[1]*, R. Lewis[1], S.E Franklin[2]
[1]The Department of Mechanical Engineering, The University of Sheffield, UK
[2]Philips Applied Technologies, Eindhoven, The Netherlands and University of Sheffield, UK

Received Date Line (to be inserted by Production) (8 pt)

Abstract

Ridges are often added to surfaces to improve grip of objects such as sports equipment, kitchen utensils, assistive technology, etc. Although considerable work has been carried out to study finger friction generally, not much attention has been paid to understanding and modelling the effects of surface texture. Previous studies indicate that at low roughness values friction decreases as roughness increases, but then a sharp increase is seen after a threshold level of roughness is reached. This is thought to be due to interlocking. In this study an analytical model was developed to analyse the different mechanisms of friction of a fingerpad sliding against triangular-ridged surfaces that incorporated adhesion, interlocking and hysteresis. Modelling was compared with experimental results from tests on five different triangular-ridged surfaces, manufactured from aluminium, brass and steel. Model and experiment compared well. The study showed that at low ridge height and width the friction was dominated by adhesion. However, above a ridge height of 42.5 μm, interlocking friction starts to contribute greatly to the overall friction. Then at a height of 250 μm, a noticeable contribution from hysteresis, of up to 20 % of the total friction, is observed.

Keywords: kinetic friction, ploughing friction, adhesion.

*Corresponding author. Tel.: +44 1142227839; fax: +44 1142227890.
E-mail address: m.j.carre@shef.ac.uk (M.J. Carré)

Nomenclature

A	Real area of contact
a	Longest distance from centre-line of ridge to contact with skin
a_H	Radius of contact predicted by Hertz
E	Young's modulus
F	Friction force
F_a	Adhesive Friction force
F_{hys}	Hysteresis Friction force
F_i	Interlocking Friction force
h_{ridge}	Height of ridge
h_{sing}	Depth of deformation for a single ridge contact
h_{adj}	Depth of deformation when there is an adjacent ridge in contact
L	Length of the ridge contact
n	Number of ridges in contact
N	Applied normal load
N'_{pr}	Equivalent normal load per ridge
p	Pressure along the contact area of the ridge and skin
R	Radius of undeformed finger
α	Pressure coefficient
β	Fraction of elastic energy lost due to hysteresis
λ	Distance between ridge peaks
θ	Angle between the side of the ridge or indenter and the vertical centre line
τ_0	Intrinsic interfacial shear strength

1. Introduction

Ridges are often added to surfaces to improve grip of objects such as; sports equipment, kitchen utensils, assistive technology, aids, etc. Although considerable work has been carried out to study skin friction, there is very little work in the literature to suggest how these ridged patterns affect friction or how any effects can be modelled (for an overview see for example [1, 2]). A survey as part of a previous study [3] examined a wide range of textures found on 69 typical handheld objects including, amongst other things, food packaging and household utensils. Texture designs fell into four main categories; criss-cross patterns, dimples, pimples and ridges. The most common category was a ridge pattern, either triangular or rectangular in cross-section and between 0.1 to 5.0 mm in height. This paper is concerned with fine surface textures that have triangular ridges at the small end of this spectrum, ranging from 0.003 to 0.26 mm in height.

Many important aspects of finger friction have been well investigated. Studies examining the effect of load [4, 5], have shown that above a normal load of around 1 N, contact area plateaus and the adhesion mechanism dominates finger friction on smooth surfaces made from various metals, polymers and glass. Other studies concerned with the presence of moisture, have postulated that water absorption, possibly together with capillary adhesion can cause increased adhesion friction due to an increase in contact area [6] and that moisture can also cause a "stick-slip" feeling for a rubbing contact between a finger and artificial skin [7]. A study on the effect of contact pressure, showed that for contact situations where the adhesion mechanism dominates, friction coefficients decreased with increasing contact pressure, but if deformation played an important role, contact pressure had less of a measureable effect [8].

Previous studies on the effect of surface roughness on friction include one that measured friction between the finger and 21 different grades of paper (Ra values ranging from 1.2 to around 4.0 μm) and found that the rougher papers had a lower friction coefficient than the smoother papers [9]. Hendricks & Franklin studied Ra values from 0.1 to around 10 μm for metals and polymers and showed that at these levels of roughness, friction when in contact with forearm skin decreased as Ra went up (see Figure 1) [10]. This was thought to be due to the decrease in contact area that would be seen at higher roughness. Clearly the situation for the finger will be different to other areas of the body at higher roughness values due to the higher roughness brought about by the ridge pattern (values of Rq have been reported between 7 and 17μm [3]). Another study by Derler et al. examined index fingerpad (mean Rz values between 62 and 99 μm) and edge of hand contacts (mean Rz values between 33 and 73 μm) with smooth glass (Rz = 0.05 ± 0.01 μm) and rough glass (Rz = 45.0 ± 5.6 μm) [8]. As with the study by Hendricks & Franklin [10], they found that under dry conditions, friction coefficient decreased with surface roughness (for both fingerpad and hand).

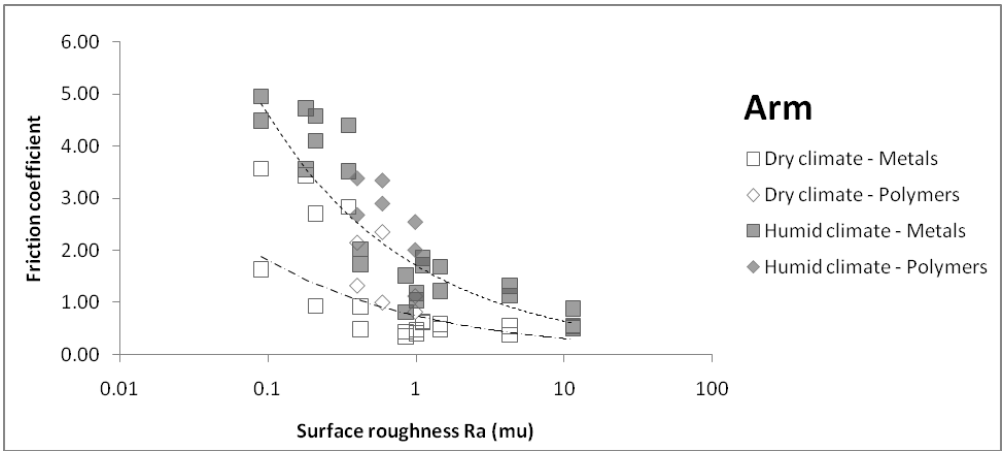

Fig. 1. Friction as a Function of Roughness for Forearm Skin (taken from [10])

One study involving larger scale texture [11] investigated the effect of rectangular cross-section ridges (made from polycarbonate) on friction. The ridge height was 0.5 mm, and the ridge width and groove width ranged from

0.5 mm to 1.5 mm. The tests were done on 14 male volunteers in ambient conditions, and it was also found that the friction decreased when ridges were added to the surface. This was attributed to a lower area of contact, and therefore less adhesion.

Tomlinson et al. [4], however, showed that for surfaces with triangular ridges (giving roughness values up to 100 μm – see Figure 2 for examples of 2D profiles) a threshold existed above which friction increased. This was thought to be due to the initiation of interlocking of the ridges on the finger pad. The friction data is shown in Figure 3. Interestingly, closer examination of the data at lower roughness indicates that friction remained relatively stable rather than decreasing as seen in work with surface textures without "directionality". It may be that for this type of surface texture the interlocking actually initiates at relatively low values of roughness and then has an increasing effect as roughness rises.

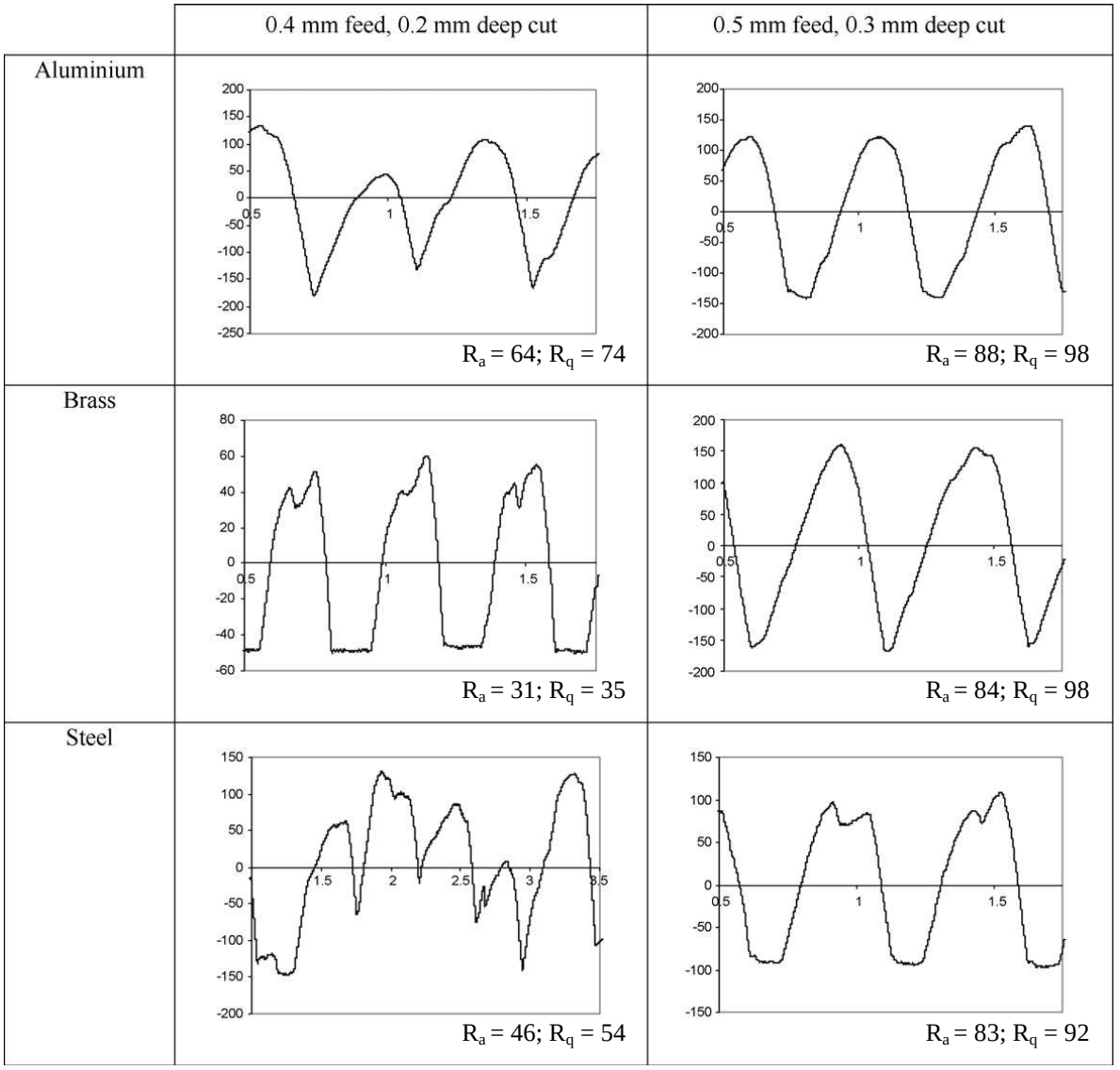

Fig. 2. Profiles of Aluminium, Brass and Steel at 0.4 mm feed, 0.2 mm cut and 0.5 mm feed, 0.3 mm cut. Ridge height is in μm, width is in mm, roughness values are in μm (taken from [4])).

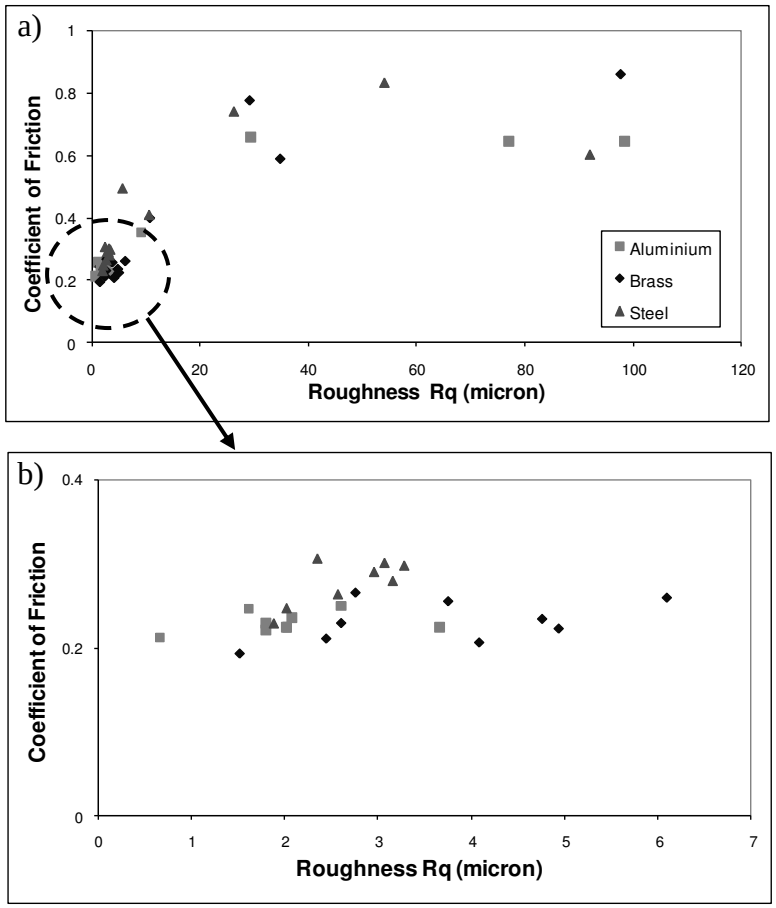

Fig. 3. Friction versus Roughness for a range of materials with triangular ridges (taken from [4]) – a) All data; b) Data for surfaces with low roughness values.

Tests were carried out on aluminium (HE 30), brass (CZ 121) and steel (S 275). A shaping machine was used to put thin horizontal grooves in the metal. The tool used was a 60° point tool, and the grooves were machined at 0.5 mm feed, 0.3 mm deep cut; 0.4 mm feed, 0.2 mm deep cut; 0.3 mm feed, 0.15 mm deep cut; 0.2 mm feed, 0.1 mm deep cut; and 0.1 mm feed, 0.05 mm deep cut.

Given the limited work in the literature on this subject there is clearly a need for more to be done in this area, particularly modelling, to provide a basis for improved grip design.

One major driver for this is safety. In 2007/2008 there were 43,518 reported accidents at work due to handling, lifting or carrying [12]. If the grip on these products can be optimised, it is hoped that some of these accidents can be prevented. In addition to safety aspects, improved grip can also enhance the performance of products, such as in sports equipment, or enable a larger group of people to use a product. For example; if screw

top bottles are easier to open, more independence could be given back to the elderly, who often struggle to open them.

The objective of this work was to advance the findings of the previous work on triangular ridges by Tomlinson et al. [4] and develop an analytical model for friction that could provide a basis for designing more effective surface textures for good grip.

2. Analytical Model Development

Previous work analysing skin friction has suggested that there are two principle mechanisms; adhesion and hysteresis friction [13]. For a finger contacting a flat surface, hysteresis is said to be negligible [4, 14] and this was also found for a sphere contacting a forearm [15]. However, in the tests carried out with triangular ridges [4], the presence of ridges introduced hysteresis as an additional component of friction, so both mechanisms must be analysed as well as the interlocking mechanism thought to cause the rise in friction with roughness. The aim here was to develop a model to compare against the experimental results presented in Figure 3 for fingerpad sliding contacts with triangular ridges in aluminium, brass and steel.

2.1. Adhesive Friction

The adhesive friction force (F_a) for a spherical probe contacting a forearm can be described using Equation 1 [13].

$$F_a = \tau_0.A + \alpha.N \quad (1)$$

where A is the real area of contact, N is the applied normal force, τ_0 is the intrinsic interfacial shear strength and α is a pressure coefficient. The coefficients τ_0 and α for the tested finger on the nominally flat surfaces of brass, steel and aluminium, can be taken from previous experiments [4], and are shown in Table 1. If it is assumed that Equation 1 is applicable to a ridged surface, the average pressure distribution can be used and the adhesive friction can be calculated. The apparent area of contact can be calculated using Hertz contact theory and an assumed radius of the finger (16 mm) (which is the radius, considering the spherical profile from the finger to interphalangeal joint, of the test finger) and also increasing the contact radius in one direction, due to the addition of ridges to the surface. The real area is then assumed to be half the apparent contact area, based on previous studies [3].

Table 1. The adhesive friction coefficients for each material at the surface roughness shown (taken from [3])

Material	**R_q (µm)**	**τ_0 (N/m^2)**	**α**
Aluminium	1.62	5479	0.24
Brass	1.71	4870	0.21
Steel	1.44	2254	0.23

2.2. Hysteresis Friction

Greenwood and Tabor [16] formed a model for hysteresis friction of a rigid conical slider along a rubber or a soft elastomer. This is shown in Equation 2. Their method of derivation was used and adapted to derive the hysteresis friction for a finger contacting a triangular ridged surface.

$$\mu_{\mathrm{h}} = \frac{\beta}{\pi} \cot \theta \tag{2}$$

where μ_{h} is the coefficient of friction due to hysteresis alone, β is the fraction of elastic energy lost due to hysteresis, and θ is the angle the side of the conical indenter makes with the vertical centre line.

To estimate the hysteresis friction for this case, a single triangular ridge was considered; Figure 4 shows an illustration of the ridge-skin contact. The skin is only displaced by the leading edge, so the deformation force is only along this side of the ridge; however, the normal force is applied to the whole ridge.

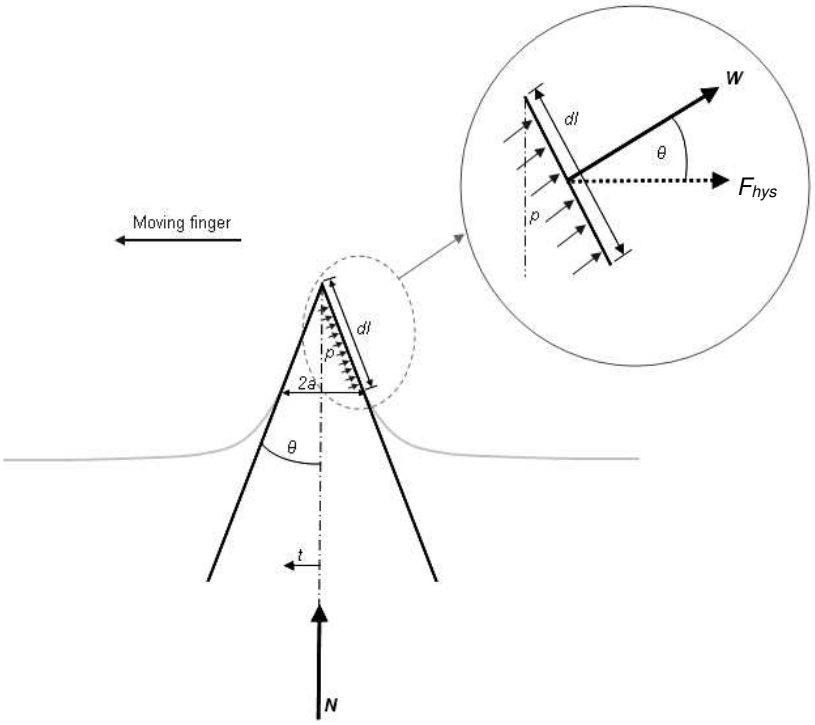

Fig. 4. Schematic of a single ridge contacting the finger pad (N is the normal force, t is the distance from the centre line of the ridge, θ is the angle of ridge, a is the largest distance from centre line to contact of the ridge with the skin, p is the pressure along the contact area of the ridge and skin, dl is the length of the contact area, W is the resultant force due to applied pressure and F_{hys} is the deformation force)

There will be a pressure along the leading edge, which varies along the length dl. The force (W) due to the pressure of the ridge pressing against the skin is:

$$W = \int p \cdot L \cdot dl \tag{3}$$

where L is the length of the ridge contact normal to the plane of the paper.

Equation 3 can be re-written (see Equation 4), since the distance from the central axis (t) varies such that dt = *dl.sinθ*. Integrating this between the limits of 0 and a, accounts for the contact area (since a is the distance t where the skin leaves contact with the ridge).

$$W = \int_0^a \frac{p \cdot L}{\sin\theta} dt \tag{4}$$

The hysteresis force due to deformation (F_{hys}) is the horizontal component of the force due to the applied pressure (W). Equation 5 describes this force.

$$F_{hys} = W \cdot \cos\theta = \int_0^a p \cdot L \cdot dt \cdot \cot\theta \tag{5}$$

The normal force (N) is described using Equation 6.

$$N = 2\int_0^a p \cdot L \cdot dt \tag{6}$$

Therefore the deformation force can be described using Equation 7.

$$F_{hys} = \frac{N}{2} \cdot \cot\theta \tag{7}$$

There will, however, be a limit to this friction, since the finger can only deform so far, and the ridge is not of infinite height. The ridges tested were not tall, and therefore the finger's maximum deformation is not reached, thus the ridge height is the limiting factor.

The model of a single ridge does not fully describe the deformation force, since the adjacent ridges restrict the finger from fully deforming. To take this into account, an equivalent applied load (*N'*) can be calculated and used to replace N in Equation 7.

To calculate the equivalent load, it was assumed that the finger deformation is symmetrical and can therefore be estimated (in 2D) using circles (post ridge contact). This physically means that when the whole finger deforms due to contact with a ridge, at the point of leaving the ridge it forms an arc. This arc can be modelled by a circle at a tangent to the ridge (the tangent being the point at which the finger surface leaves contact with the ridge). This is illustrated in Figure 5. In this figure the larger circle represents the finger that is deforming on a single ridge, and the smaller circle represents the deformation of the finger when there is an adjacent ridge.

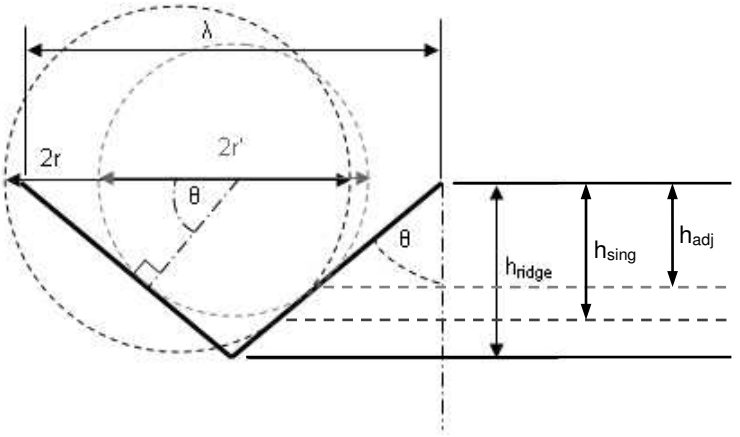

Fig. 5. Schematic of the Circular Representation of a Finger Deforming on a Ridge (r = radius of the circle without an adjacent ridge and *r'* = radius of circle with adjacent ridge)

When Figure 5 is drawn to scale, it can be seen that the ratio of the circle radii is equal to the ratio of deformation depths. The deformation depths are considered to be from the tip of the ridge point to the tangent of the circle with the ridge. For a single ridge contact, the depth of deformation (h_{sing}) can be estimated using Hooke's Law, as shown in Equation 8 (for loads above 2 N, after which the majority of the fingerpad has deformed and area of contact plateaus for contacts with flat surfaces [3]). This assumes the rough approximation that the spring constant (k) is linear and since the finger is pre-compressed this assumption is believed to be appropriate for this model [3].

$$h_{sing} = \frac{N}{k} \tag{8}$$

The ratio of the radii to the finger deformation can then be rearranged to give an equation for the depth of deformation (h_{adj}), when there is an adjacent ridge.

$$h_{adj} = \frac{r'}{r} \cdot h_{sing} = \frac{\left(\frac{\lambda}{2} \cdot \cos\theta\right)}{h_{ridge}} \cdot h_{sing} = \frac{\lambda \cdot \cos\theta}{2 \cdot h_{ridge}} \cdot h_{sing} \tag{9}$$

Again applying Hooke's law, an equivalent load can be calculated for the new modified deformation, described by Equation 10.

$$N' = k \cdot \frac{\lambda \cdot \cos\theta}{2 \cdot h_{ridge}} \cdot h_{sing} \tag{10}$$

Since h_{sing} can be estimated using Hooke's law (Equation 8), the overall equivalent load per ridge (N'_{pr}) can be described using Equation 11.

$$N'_{pr} = \frac{N}{n} \cdot \frac{\lambda \cdot \cos\theta}{2 \cdot h_{ridge}} \tag{11}$$

where n is the number of ridges in contact.

This equivalent load can then be used as the input to compare whether maximum deformation has occurred yet. If it has, the limiting load, N_{max}, (the load at which the deformation reaches a maximum) is used, rather than the equivalent load. This deformation force (for a single ridge) is then multiplied by the number of ridges in the contact, to calculate the total deformation.

The number of ridges in contact is calculated using Equation 12 where $L = 2a_H$, a_H = radius of contact predicted by Hertz (Equation 13).

$$n = \frac{L}{\lambda} \tag{12}$$

$$a_H = \left(\frac{3 \cdot N \cdot R}{4 \cdot E^*} \right)^{1/3} \tag{13}$$

The deformation force is an overestimate of the hysteresis friction (F_{hys}), since the skin is able to return to its original shape, which is a mechanism of energy return. However, the visco-elastic nature of the skin means that not all of the energy inputted to deform the skin is recovered. This difference can be represented by the viscoelastic hysteresis loss fraction, β. Therefore, by rewriting Equation 7 to replace N with the total equivalent load N' (= n N'_{pr}), combining it with Equation 11 and taking into account the loss fraction, β, the overall hysteresis friction can be calculated as shown in Equation 14. The loss fraction is dependent upon loading and unloading rate, so will vary between ridge patterns, and can be found experimentally.

$$F_{hys} = \begin{cases} \beta \cdot N \cdot \dfrac{\lambda \cdot \cos\theta}{4 \cdot h_{ridge}} \cdot \cot\theta & N'_{pr} < N_{max} \\ \beta \cdot n \cdot \dfrac{N_{max}}{2} \cdot \cot\theta & N'_{pr} \geq N_{max} \end{cases} \quad (14)$$

2.3. Interlocking Friction

Considering the friction between a steel indenter and a nitrile rubber [17], past a certain level of roughness (R_a = 1.6 μm for the rubber and R_a = 1.88 μm for the steel) interlocking of the asperities causes an increase in friction. The ridged surfaces in question for our model validation are a higher roughness than this (R_a = 0.98 – 82.73 μm; R_q = 1.19 – 98.42 μm), and the roughness of the finger is R_q = 7 – 17 μm [3] (the height of ridges varies across the finger pad). This means an additional mechanism of friction could be the fingerpad ridges 'climbing' over the metallic surface ridges leading to interlocking friction. Adams [18] estimated the coefficient of friction due to interlocking, of one spherical particle climbing over another spherical particle, to be equal to the tangent of the angle between the normal force and the vertical. This calculation can be repeated for the finger ridges 'climbing' an incline with the same result; thus interlocking friction can be described using Equation 15. It is assumed that the total friction force, will result from a total normal load, even if this load is applied over a number of fingerpad ridge-surface ridge interactions.

$$F_i = N \cdot \cot\theta \quad (15)$$

Finally, the total friction can be found simply as

$$F = F_a + F_{hys} + F_i \quad (16)$$

3. Modelling Results

Assuming a loss fraction of 0.45 [19], and using Equations 1, 14 and 15, the friction force for a finger contacting a triangular ridged surface can be predicted. Figure 6 shows the predicted and measured values of frictional force for the materials tested. Data is presented for three materials, each having been used to create five different fine-ridged surfaces and each surface having been tested at five different normal loads (giving 75 data points in all). Tests were carried out using one participant (female, 25yo), where the middle finger of the dominant hand was drawn across the surface, in a direction perpendicular to the ridge pattern [4].

There is a fairly good correlation between the predicted and measured values for the brass samples, both in terms of accuracy and precision (i.e., both the slope and correlation coefficient are relatively close to unity). The profiles for brass (see Figure. 2) can be seen to be closest to the assumed triangular pattern, which may explain why the model gave the best predictions for this material. However, Figure 6 indicates that there was less accuracy in the predicted values of friction for the other materials, steel and aluminium, as the slopes were less

close to unity. The low slope values indicate that, generally, the model overpredicted the friction forces for steel and aluminium. It is hypothesized that this overprediction is based on the assumption that the ridges had distinct, sharp points, leading to the assumed values of interlocking friction, whereas in reality (see Figure 2), the ridges for steel and aluminium were slightly blunt. The predictions for steel were the least precise (indicated by the low correlation coefficient) and this is thought to be due to the inconsistent profile of the steel ridges, particularly for samples with low ridge height (see Figure 2).

There are also likely to be errors in some of the other assumptions made, such as the single assumed loss fraction, and assuming the adhesion equation for a flat surface can be applied to ridges, and using the interlocking equation for a particle, since this may be reduced for the skin due to its visco-elastic nature.

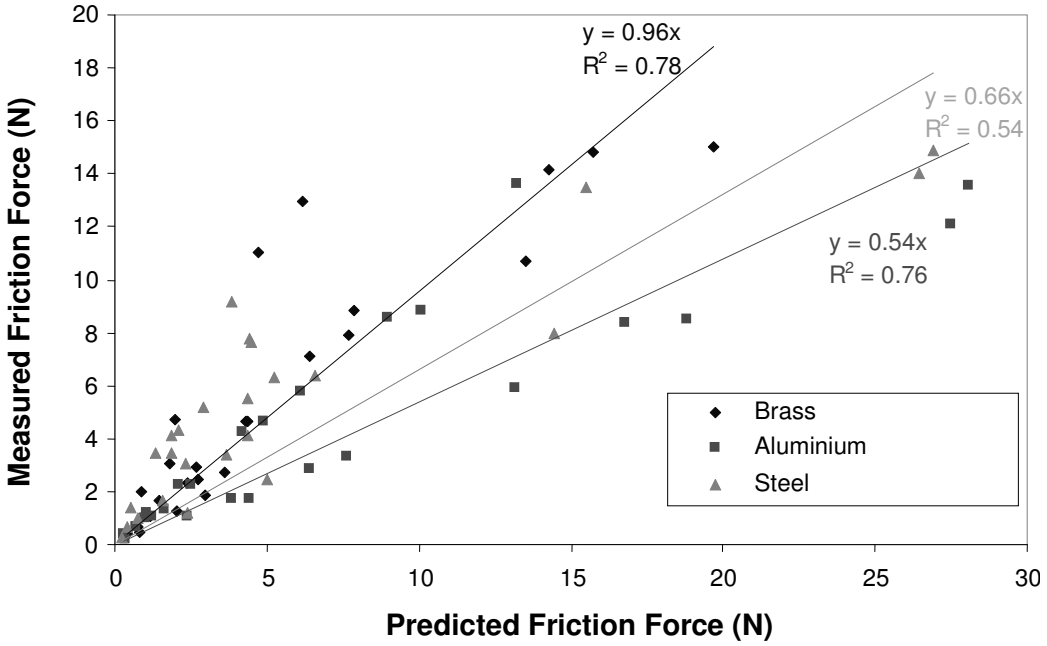

Fig. 6. Comparison of Predicted Friction Force and the Measured Friction Force, for the Ridge Patterns

The modelling results also allow an analysis of which mechanisms of friction are important in a particular contact, so that these can be either maximised or minimised for optimum friction properties. Figure 7 shows the predicted overall friction forces for tests done on the brass surfaces, broken down into contributions of each friction mechanism. This shows that for small ridges adhesive friction has the largest influence on the total measured friction. Once the applied loads are greater and the ridges are larger, interlocking friction starts to account for a large percentage of the overall friction. Interestingly, for the ridge dimensions chosen, hysteresis friction contributed very little to the overall friction, as seen with a previous study using a spherical indenter on the forearm [15].

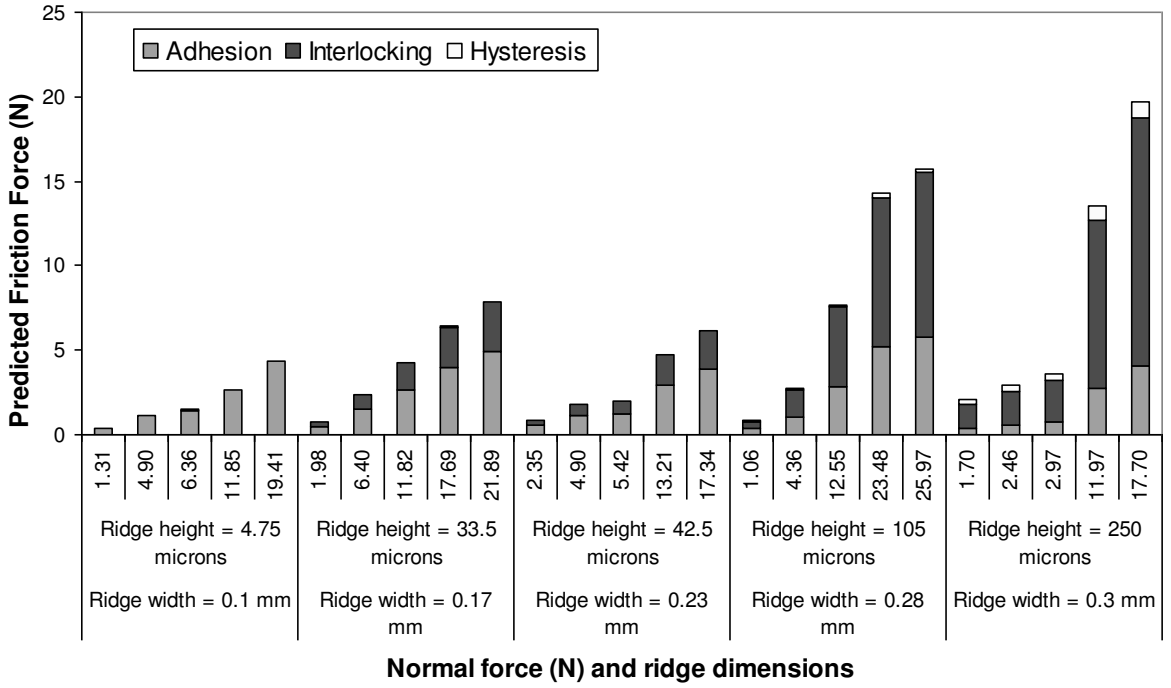

Fig. 7. Contribution of each mechanism to the overall predicted friction for brass surfaces

4. Discussion

4.1. Mechanisms of Friction

The experimental data in Figure 3 indicates that the coefficient of friction plateaus with roughness, however, prediction made from the analysis of the different friction mechanisms do not support this (see Figure 8). This was investigated further by analysing the different friction mechanisms as the finger moves over a fine ridged surface.

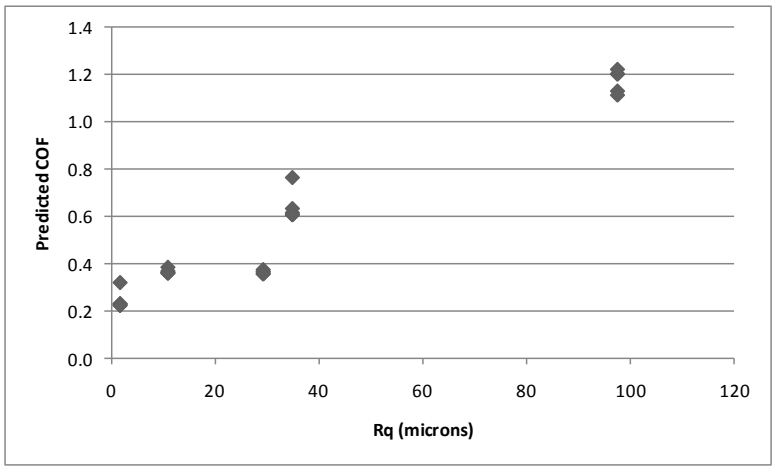

Fig. 8. Predicted Coefficient of Friction against roughness for brass surfaces

Figure 7 shows that at low ridge height, adhesion is the most dominant friction mechanism. This is because the surface profile is such that the ridges do not penetrate a great deal into the surface of the finger. At a greater height and width, there is more penetration into the finger, therefore the amount of hysteresis friction increases.

The main increase in friction, as the size of the ridges is increased, is due to interlocking friction. Interlocking friction is mentioned by Chang et al. as contributing to rubber friction [20], but no models were applied in this study. In examining existing models, it was found that Adams's model of a particle 'climbing' over another particle can be applied [18]. This shows that if the angle of the ridge is sharper, there will be a greater amount of interlocking friction. In application of the interlocking equation, the constraint was used, such that the amount of interlocking was calculated as a percentage of the number of metallic ridges larger than the finger ridges. This is based upon the fact that interlocking friction is usually observed when the dimensions of an asperity are greater than those of the contacting asperity [21].

4.2. Results in Terms of Surface Design and Work for the Future

A comparison of Figures 7 and 8 shows that there is very little difference in the coefficients of friction (friction force divided by normal force) for each texture, until a width of 0.28 mm and height of 108 μm, where there is an increase in friction. There is a substantial increase for the surface with ridges of 0.3 mm width and 250 μm height. This shows that if designing a surface for the maximum friction, the larger and higher the ridges, the better. There may of course be a limit to this height, which has not been investigated as part of this study.

In the design of grips, comfort is also important. A perception study would add to the understanding developed in this paper, using the type of techniques outlined in the work of Barnes et al. [22]. This could then provide a full catalogue of information for grip design. This work can be improved and furthered, by looking at a wider range of ridge heights and widths. Also, a better manufacturing method would ensure that the profiles were regular. This would allow better comparison of the results to the model, thus providing a better picture of the mechanisms of friction present, and how the ridge shapes affect friction.

5. Conclusions

In this study a model was developed for addressing finger-texture contact and predictions from the model were compared to experimental values.

In the cases modelled, adhesion was the predominant mechanism (responsible for more than 50% of the total friction force, and in some cases, up to 100%) for samples with shallow ridges of a height lower than 42.5 μm (note: the spacing of the ridges also has an effect, but for the samples used in this study, ridge height was the main parameter that dictated the shallowness or sharpness of the ridges). This is because the ridges are so shallow, they allow a relatively large contact area, and therefore adhesion. However, for the samples with ridge heights greater than 42.5 μm (and therefore sharper ridges), the interlocking friction mechanism becomes more influential, accounting for more than 50% of the total friction force. The finger ridges, are now required to 'climb' over the metallic surface ridges to a greater extent. Finally, at a height of 250 μm, hysteresis starts to play a greater part in

friction as the ridges deform the skin to a greater extent; however, this is still not a dominant mechanism (responsible for no more than approx. 10% of the total friction force).

References

[1] S. Tomlinson, R. Lewis, M.J. Carré, Review of the frictional properties of the finger-object contact when gripping. Proc. IMechE Part J: Engineering Tribology. 221 (2007) 841-850.

[2] R.K. Sivamani, J. Goodman, N.V. Gitis, H.I. Maibach, H.I., 2003, Coefficient of Friction: Tribological Studies in Man - An Overview, Skin Research and Technology, 9 (2003) 227-234.

[3] S.E. Tomlinson, Understanding the friction between human fingers and contacting surfaces, PhD thesis, University of Sheffield, UK, 2009.

[4] S.E. Tomlinson, R. Lewis, M.J. Carré, The effect of normal force and roughness on friction in human finger contact, Wear, 267 (2009) 1311-1318.

[5] A. Ramalho, C.L. Silva, A.A.C.C. Pais, J.J.S. Sousa, In vivo friction study of human skin: influence of moisturizers on different anatomical sites, Wear, 263 (2007)1044-1049.

[6] S. Tomlinson, R. Lewis, X. Liu, C. Texier, M.J. Carré, Understanding the friction mechanisms between the human finger and flat contacting surfaces in moist conditions, Tribology Letters (2010) - in press.

[7] Y. Nonomura, T. Fujii, Y. Arashi, T. Miura, T. Maeno, K. Tashiro, Y. Kamikawa, R. Monchi, Tactile impression and friction of water on human skin, Colloids and Surfaces B: Biointerfaces, 69 (2009) 264-267.

[8] S. Derler, L.-C. Gerhardt, A. Lenz, E. Bertaux, M. Hadad, Friction of human skin against smooth and rough glass as a function of the contact pressure, Tribology International, 42 (2009) 1565-1574.

[9] L. Skedung, K. Danerlov, U. Olofsson, M. Aikala, K. Niemi, J. Kettle, M.W. Rutland.: Finger friction measurements on coated and uncoated printing papers, Tribology Letters, 37 (2010) 389-399.

[10] C.P. Hendriks, S.E. Franklin, Influence of surface roughness, material and climate conditions on the friction of human skin, Tribology Letters, 37 (2010) 361-373.

[11] O. Bobjer S.-E., Johansson, S. Piguet, Friction between hand and handle. Effects of oil and lard on textured and non textured surfaces; perception of discomfort, Applied Ergonomics, 24 (1993)190-202.

[12] Health and Safety Executive, Health and Safety Statistics, Statistics on work-related ill-health, injuries, dangerous occurrences, enforcement and gas safety. www.hse.gov.uk, 2008.

[13] M.J. Adams, B.J. Briscoe, S.A. Johnson, Friction and lubrication of human skin, Tribology letters 26 (2007) 239-253.

[14] C. Pailler-Mattéi, H. Zahouani, Analysis of adhesive behaviour of human skin in vivo by an indentation test, Tribology International 39 (2006)12-21.

[15] M. Kwiatkowska, S.E. Franklin, C.P. Hendriks, K. Kwiatkowski, Friction and deformation behaviour of human skin, Wear, 267 (2009) 1264-1273.

[16] J.A. Greenwood, D. Tabor, The friction of hard sliders on lubricated rubber: The importance of deformation losses. Proceedings of the Physical Society 71 (1958) 989-1001.

[17] S.J. Jerrams, Friction and adhesion in rigid surface indentation of nitrile rubber. Materials and Design, 26 (2004) 251-258.

[18] M.J. Adams, Friction of granular non-metals, in: I.L. Singer, H.M. Pollock (Eds.), Fundamentals of friction: Macroscopic and microscopic processes vol. 220. Springer, 1991. pp.183-209.

[19] T.C. Pataky, M.L. Latash, V.M. Zatsiorsky, Viscoelastic response of the finger pad to incremental tangential displacements. Journal of Biomechanics, 38 (2005) 1441-1449.

[20] W.-R. Chang, R. Grönqvist, S. Leclerco , R. Myung, L. Makkonen, L. Strandberg, R.J. Brungraber , U. Mattke, S.C. Thorpe, The role of friction in the measurement of slipperiness, Part 1: Friction mechanisms and definition of test conditions, in: W.-R. Chang, T.K. Courtney, R. Grönqvist, M.S. Redfern (Eds.), Measuring Slipperiness. Human Locomotion and Surface Factors. CRC Press, 2003. pp.119-129.

[21] B. Bhushan, Principles and applications of tribology. United States of America: Wiley - Interscience, 1999.

[22] C.J. Barnes, T.H.C. Childs, B. Henson, C.H. Southee, Surface finish and touch - a case study in a new in human factors tribology, Wear, 257 (2004) 740-750.